Lab report on

V10 – Particle identification with a ΔE-E-setup

Group Ma-A-07

Daniel Klostermann(d_klos04@uni–muenster.de)
Alexander Neuwirth(a_neuw01@uni–muenster.de)
Alex Oster(a_oste16@uni–muenster.de)

Date of experiment: 21.10.2019
supervised by Ailec de la Caridad Bell Hechavarria

December 19, 2019

Contents

1 Abstract

For this lab report the energy-loss of radiation will be observed to determine the thickness of various components. Furthermore the characteristic energy-loss of the radiation allows identification of its type, here specifically the α-radiation. In particle physics this method is often used, notably for accelerator experiments.

2 Theory

Before discussing the experiment itself, it is necessary to first understand the underlying physics. Thus, this section will serve as an introduction to α-decay, interaction of the radiation with matter as described by the Bethe-Bloch-formula as well as semi-conductor detectors, which were used for the measurement.

2.1 α-decay

The α-decay can be described as the emission of an α-particle from a mother nucleus. In itself the emitted particle is nothing more than a helium nucleus. One can describe the process as follows:

$$ {}^{A}_{Z}\mathrm{X} \rightarrow {}^{A-4}_{Z-2}\mathrm{Y} + {}^{4}_{2}\mathrm{He}, \tag{2.1} $$

where X represents the mother nucleus with mass number A and atomic number Z. Since the nucleus loses two protons and to neutrons, the leftover nucleus Y has a mass number which is lower by four and an atomic number which is lower by two.
To understand why the decay happens, the model of potential wells for protons and neutrons is of importance. This is shown in fig. 1. There one can see that the decay itself is realized through the tunneling effect. The barrier which has to be surpassed is the coulomb-wall of the mother nucleus. For this process to happen, it is necessary that the two protons and neutrons are energetically on high enough levels as shown in the figure. It is important to note that the tunneling through the classical forbidden regime is described by an exponential decrease of the wave function, where the argument of the exponential function is the so called Gamow-factor.

Due to the comparably large cross-section of the helium nuclei α-radiation has a high interaction rate with matter. The energy-loss caused by this type of interaction can be expressed by the Bethe-Bloch-formula.

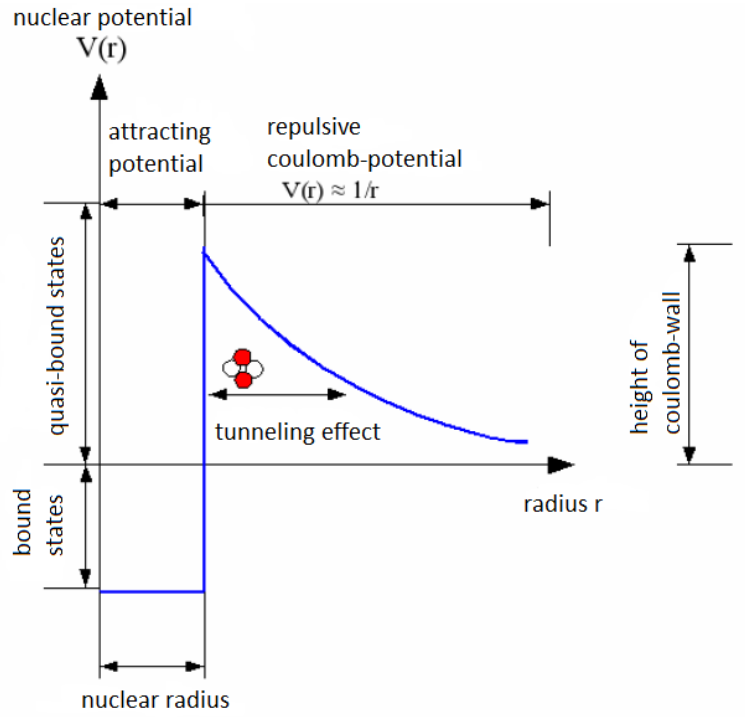

Figure 1: Schematic representation of the α-decay using the model of potential pots as well as quantum-mechanical tunneling.[1]

2.2 Interaction with matter: Bethe-Bloch-formula

To better understand which factors take part in the Bethe-Bloch-formula a short derivation follows. Starting with the simple case of a particle with mass M traveling through the Coulomb-field of another particle with a mass $m \ll M$. Because of momentum conservation there will be no change in the path of the heavier particle. Further the momentum transfer I, where the lighter particle is an electron (so $m = m_\mathrm{e}$), can be calculated

$$I = \int F \,\mathrm{d}t = e \int E_\perp \frac{\mathrm{d}t}{\mathrm{d}x}\,\mathrm{d}x = e \int E_\perp \frac{\mathrm{d}x}{v} \tag{2.2}$$

with force F acting on the particle, electric field component perpendicular to the path of the particle $E_\perp$ and elementary charge e over a Gaussian path integral:

$$I = \frac{2Ze^2}{bv}, \tag{2.3}$$

where Z is the atomic number of the heavy particle, b the distance of the electron to the path of heavy particle and v the velocity of that particle.
Thus, the energy transfer in dependency of the distance b is

$$\Delta E(b) = \frac{I^2}{2m_\mathrm{e}} = \frac{2Z^2e^4}{m_\mathrm{e}v^2b^2}. \tag{2.4}$$

Extending this to a large number of electrons via a density N_e and looking at infinitesimal changes this expression turns to

$$-\frac{\mathrm{d}E}{\mathrm{d}x} = \frac{4\pi Z^2e^4}{m_\mathrm{e}v^2}N_\mathrm{e}\ln\left(\frac{b_\mathrm{max}}{b_\mathrm{min}}\right). \tag{2.5}$$

Here the quantities $b_{\mathrm{min/max}}$ depict the minimum/maximum distance of the electrons to the path of the heavy particle.
Adding relativity and correction terms the Bethe-Bloch-formula is obtained:

$$-\frac{\mathrm{d}E}{\mathrm{d}x} = 4\pi N_\mathrm{A}r_\mathrm{e}^2m_\mathrm{e}\rho\frac{Z^2}{A}\frac{z^2}{\beta}\left[\ln\left(\frac{2m_\mathrm{e}\gamma^2v^2W_\mathrm{max}}{I^2}\right) - 2\beta^2 - \delta - 2\frac{C}{Z}\right]. \tag{2.6}$$

Table 1 lists the quantities which appear in the formula.

Table 1: List depicting the quantities in the Bethe-Bloch-formula.

r_e:	classical e^-*radius*	ρ:	density of absorbing material
m_e:	electron mass	z:	incident particle charge (in e)
N_A:	Avogadro's number	β:	v/c of incident particle
I:	mean excitation potential	γ:	$1/\sqrt{1-\beta^2}$
Z:	atomic number of absorbing material	δ:	density correction
A:	mass number of absorbing material	C:	shell correction
		W_max:	max. energy transfer in a single collision.

However the Bethe-Bloch-formula is only accurate for energies between 6 MeV to 6 GeV. For lower energies further corrections are necessary and for higher energies radiation effects have to be considered.
In fig. 2 the Bethe-Bloch-formula is displayed for Muons, which are comparably slow and therefore have much time for interactions. It shows a high rise in the energy-loss for low energies.

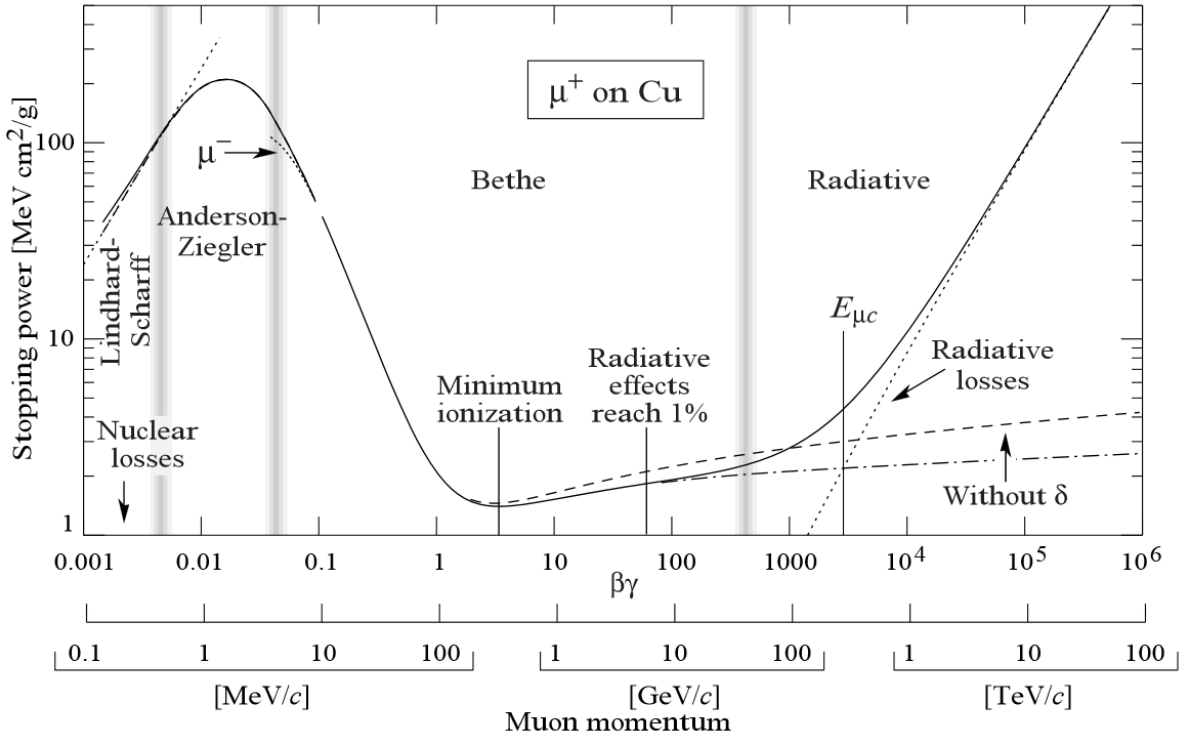

Figure 2: Schematic representation of the Bethe-Bloch-formula for Muons traveling through copper.[2]

2.3 Semi-conductor detectors

A detector of the semi-conducting type can be easily described as a diode in blocking direction. The diode itself consists of a pn-junction at which a voltage is applied. Through the polarization of this voltage one can choose whether to run the diode in blocking direction or not. This either expands or shrinks the charge-space zone at the pn-junction. Expanding it allows a larger area to interact with. An incoming particle can transfer

a part of its energy there to produce electron-hole-pairs which then diffuse to form a current. And this current is proportional to the energy of the incoming particle, which allows for conclusions to be drawn from that. The creation of electron-hole-pairs is dependent on the width of the band gap of the material. Low widths allow high energy resolution, which is a strength of semi-conducting materials compared to for example scintillation detectors.

2.4 Americium-241

The α-source which will be used in the experiment is Americium-241. Due to its lifetime of 432.2 years it is no longer acquired from nature and has to be synthesized. By Emission of an α-particle it decays into Neptunium-237. There is also the possibility of spontaneous fission, but the probability is so small, that it can be neglected. More important is the fact that the decay into Neptunium-237 only rarely leaves the nucleus in the ground state. With a probability of around 85% the decay leaves the nucleus in the second excited state. Since energy conservation holds, it is possible to deduce, which excited state remains from the energy of the α-particle.

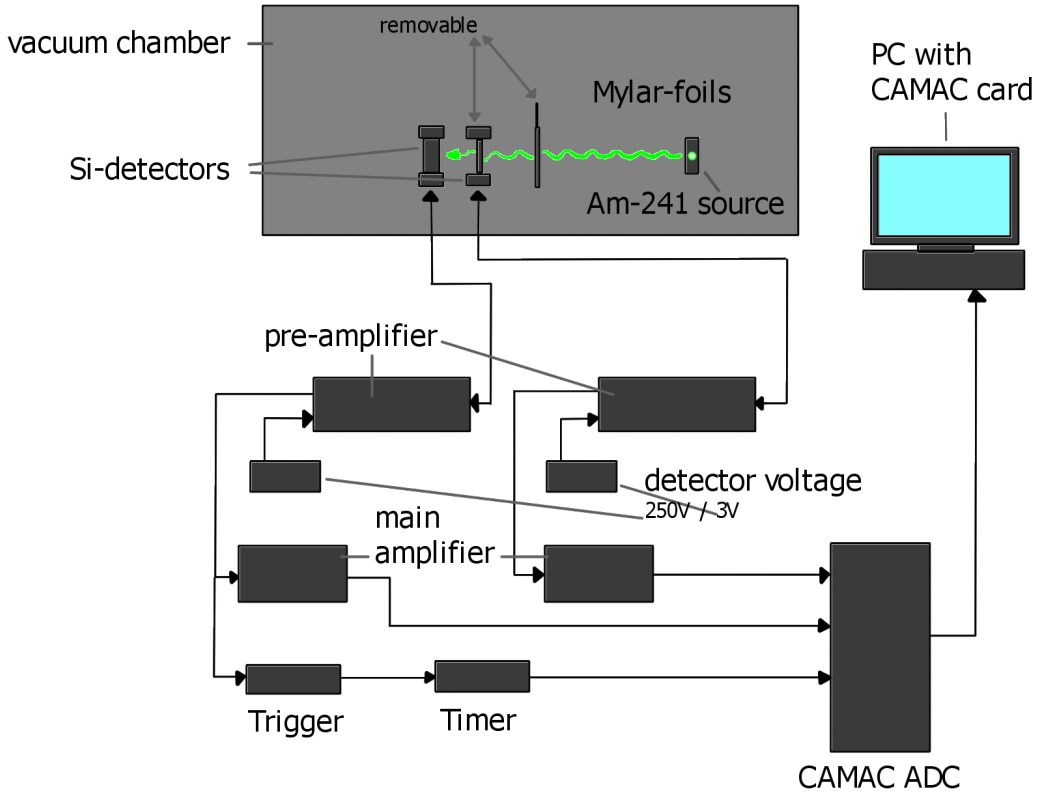

Figure 3: Schematic representation of the experimental setup.

3 Methods

The next part to look at is the experimental setup which is depicted in fig. 3. It consists of a vacuum chamber, allowing the α-particles to lose less energy than they would traveling through matter. In the chamber are the ^{241}Am-source as well as two semi-conductor detectors and three Mylar-foils. Silicon will be used for the detectors. They can be distinguished by their thickness. One will be very thin and labeled "ΔE-detector" so that the α-particles can still be transmitted through the detector without losing all their energy. The other one instead is thicker, so that the radiation will be completely absorbed there. Here the thicker detector will be called "E-detector".

To allow different types of measurement, it is possible to remove the ΔE-detector and one up to all Mylar-foils from the setup. Additionally, it is possible to turn the foils so that the radiation has to transmit through effectively more matter or rather to change the effective thickness of the foils.
Since the signals of single detection are rather low, the detectors are connected to pre- and main-amplifier. From there the signals will be read by a CAMAC ADC, where they are digitized and sorted to channels. In the following section these channels will be calibrated to be referring to specific energies. This will be done by taking the most probable α-energy and correlate it to the channel with the highest intensity. Of importance in experimental setups is the reduction of noise which is achieved here through the addition of a trigger connected to the E-detector. Furthermore, there is a timer added that allows the measurement of only coincident events in ΔE and E-detector.
The first measurement will be without the ΔE-detector and foils. So the α-energies can directly be measured without being absorbed beforehand. After this, the calibration will follow.
Going forward the thickness of ΔE-detector and foils will be determined. At first only the ΔE-detector will be inserted and the energy-loss compared with the first measurement. Through that it is possible to deduce the thickness. This will be repeated but without the ΔE-detector and instead with one, two and then three Mylar-foils at a 0° angle (so perpendicular to the incident particle beam). The exact calculations follow in the next section.
For the last measurement the ΔE-detector will be inserted again. To be exact this is not a single measurement but a series. Here at first one foil will be added and turned up to 60° in 15° steps from a 0° angle. Thereafter, a second foil will be added and again turned. The same will be repeated for the third foil and the results will be compared to the Bethe-Bloch-formula.

4 Results and discussion

In this section the data taken from carrying out the measurements, as described in the previous section, will be evaluated and then discussed.

4.1 Observations and analysis

After correctly setting up the experiment the measurements could be made without any disturbing factors. To start of with analyzing the data, the first step is the calibration of the detectors. Thereafter the determination of thickness will occur and lastly the particle identification via the Bethe-Bloch plot. For this the event rates of particles passing the foils were too low for two foils at 60° and three foils at 45° and 60°. Here it is necessary to note that the leftover energy of the particles may be too low for the trigger to activate. Therefore less events were collected in the low energy range.

4.1.1 Calibration E-detector

In fig. 4 the event count is displayed against the channel of the ADC. The uncertainties are based on a Poisson distribution and therefore $u(N) = \sqrt{N}$. Two peaks are visible and two Gaussian functions are fitted simultaneously.

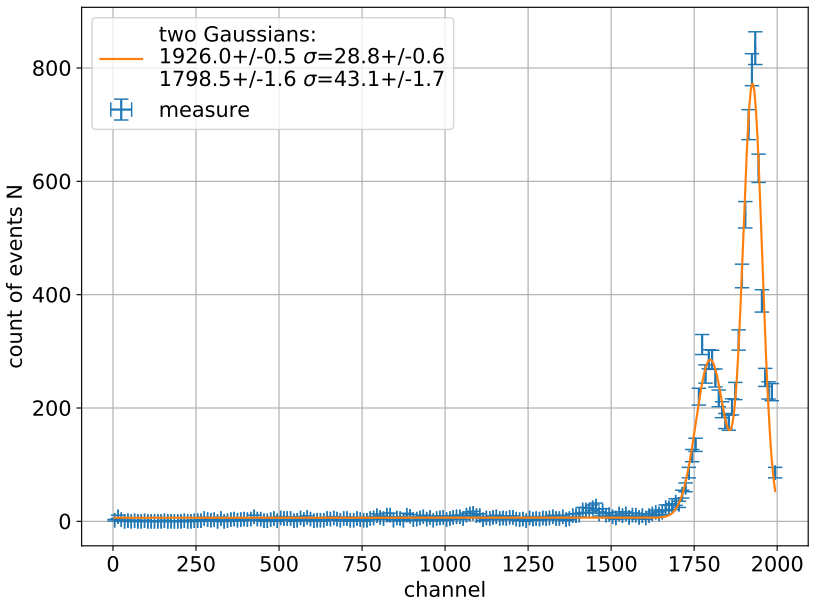

Figure 4: E-detector measure without foils and no ΔE-detector.

The dominant peak is the alpha emissions from $^{241}_{95}\mathrm{Am}_{146}$ of energy $(5416.27 \pm 0.12)\,\mathrm{keV}$ with a probability of $(84.45 \pm 0.10)\,\%$. In fig. 5 the calibration factor from channels to energy is plotted as a straight line. The channel 0 is assumed to be of energy $E = 0$.

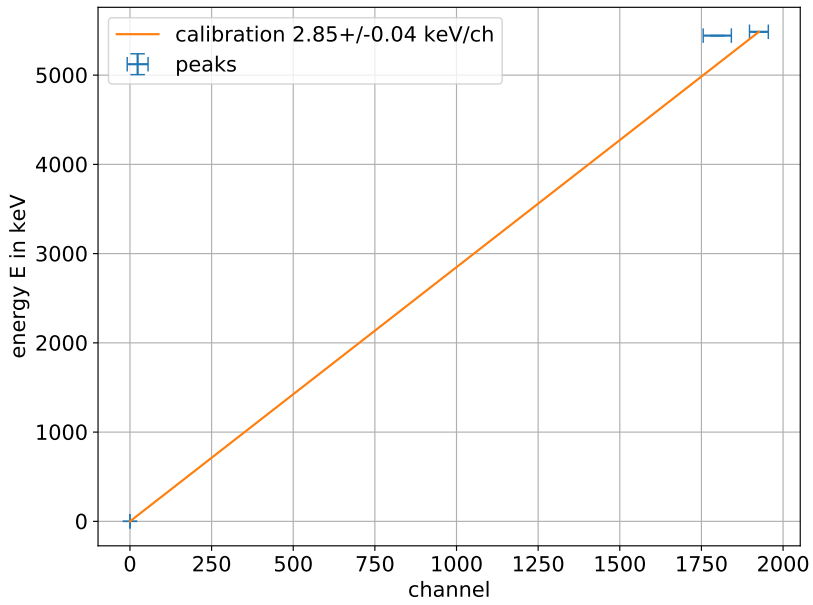

Figure 5: *E*-detector calibration curve.

The peaks are displayed with uncertainties corresponding to the standard deviations of the previous fits. For the second peak the second most dominant decay of Americium (5442 keV at 13 %) was tested, but it seems more likely that this peak overlaps with the dominant peak. The second peak might occur due to (back-)scattering effects. The fig. 6 is the same plot as before, but with an additional uncertainty on the measured kinetic energy E.

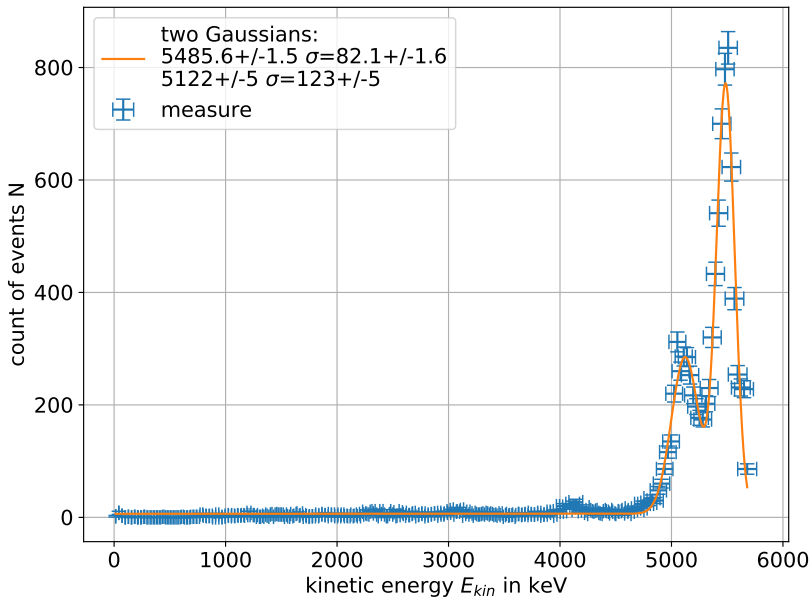

Figure 6: E-detector measure with calibration.

4.1.2 Calibration ΔE-detector

With the ΔE-detector in between the source and the E-detector a direct drop in the energy E is observed in fig. 7 compared to fig. 6. A peak is also observed in the ΔE-detector in fig. 8.

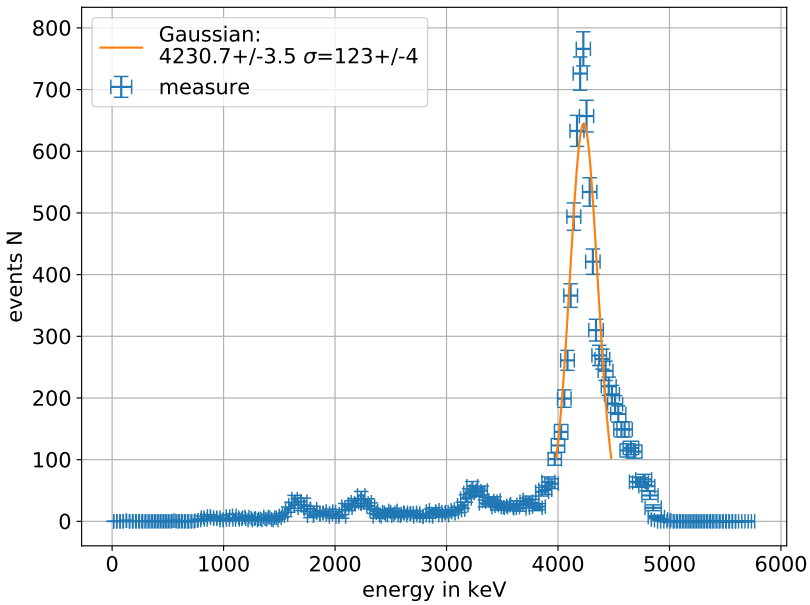

Figure 7: E-detector measure with ΔE-detector.

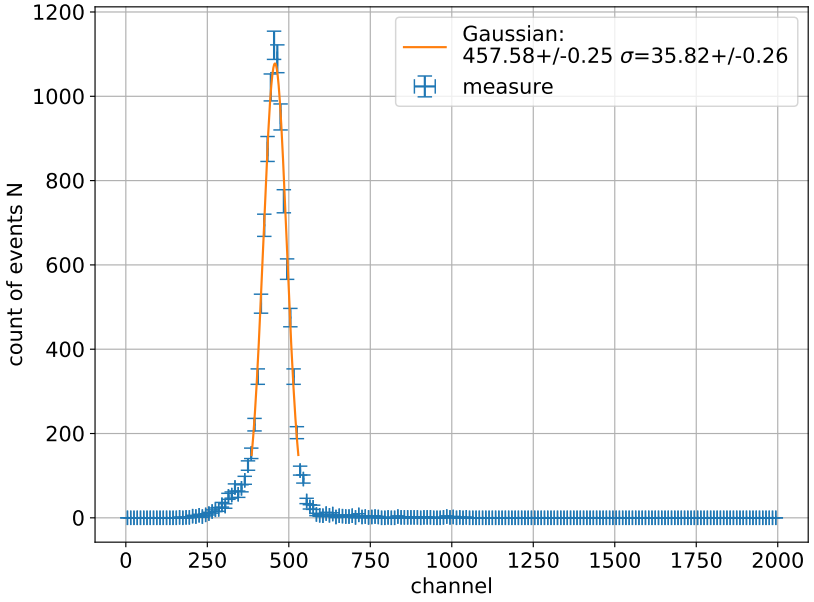

Figure 8: ΔE-detector measure.

These peaks are approximated as Gaussian. The position of this peak in the ΔE-detector can now be calibrated to correspond to the drop in energy (from fig. 6 to fig. 7) namely

the energy that is deposited in the ΔE-detector. Again a linear dependence and $E = 0$ at the zero channel are assumed. The result is fig. 9.

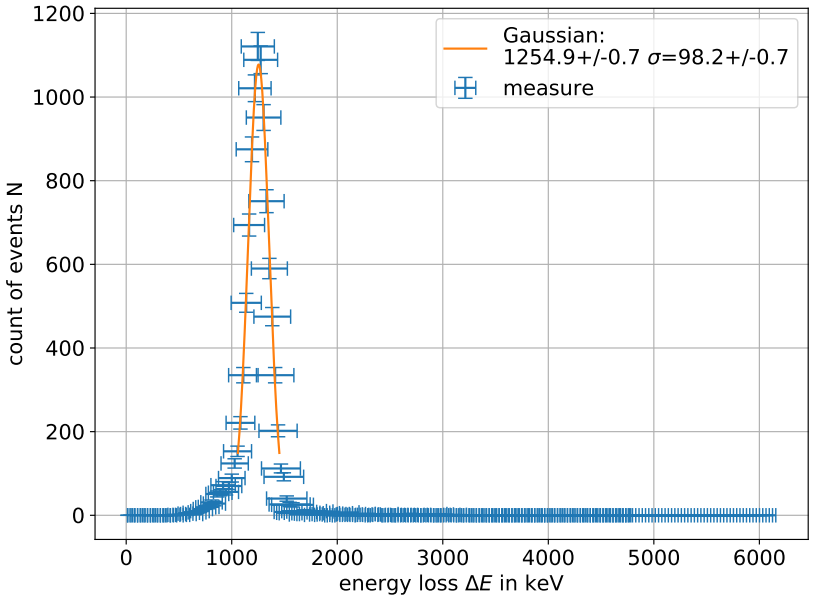

Figure 9: ΔE-detector measure with calibration.

4.1.3 Thickness measurements

In fig. 10 three E-detector measure series are listed. One for each Mylar foil constellation.

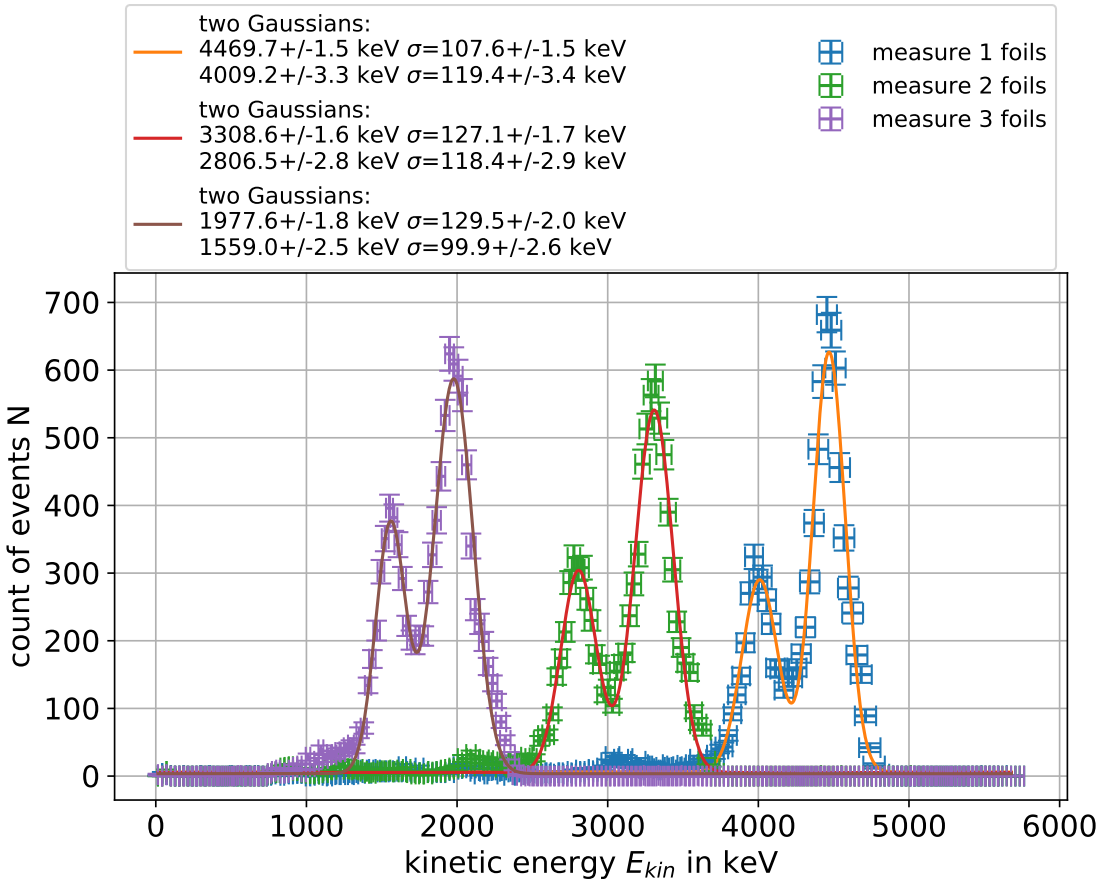

Figure 10: E-detector with different foils.

The resulting peaks are fitted so that the energy-loss ΔE can be used to calculate the thickness d of the absorbing material.
For both silicon and Mylar the energy-loss $-dE/dx$ is given for discrete steps in [3]. Here a linear interpolation is sufficient. The thickness is given by

$$d = \int_0^d dx = \int_{E(0)}^{E(d)} \frac{dx}{dE} dE = \int_{E(d)}^{E(0)} \frac{1}{-\frac{dE}{dx}} dE \,. \tag{4.1}$$

Given a range $[E_j, E_{j+1}]$ with $E_{j+1} > E_j$ the interpolation is

$$L(E) = -\frac{dE}{dx} = \frac{E(L_{j+1} - L_j) + L_j E_{j+1} - L_{j+1} E_j}{E_{j+1} - E_j} \tag{4.2}$$

satisfying

$$L(E_j) = L_j \tag{4.3}$$
$$L(E_{j+1}) = L_{j+1}\,. \tag{4.4}$$

Integration over this range gives

$$d_j = \int_{E_j}^{E_{j+1}} \frac{dE}{a_j E + b_j} = \frac{1}{a_j} \ln\left(\frac{a_j E_{j+1} + b_j}{a_j E_j + b_j}\right) \tag{4.5}$$

with

$$a_j = \frac{L_j - L_{j+1}}{E_{j+1} - E_j} \tag{4.6}$$
$$b_j = \frac{L_j E_{j+1} - L_{j+1} E_j}{E_{j+1} - E_j}\,. \tag{4.7}$$

With an initial energy $E_{n+1} > E_i > E_n$ and a final energy $E_1 > E_f > E_0$ the whole thickness is

$$d = \frac{1}{a_n} \ln\left(\frac{a_n E_i + b_n}{a_n E_n + b_n}\right) + \sum_{j=1}^{n-1} d_j + \frac{1}{a_0} \ln\left(\frac{a_0 E_1 + b_0}{a_0 E_f + b_0}\right)\,. \tag{4.8}$$

The initial energy $E_i = 5416\,\text{keV}$ is known from the calibration and E_f is given by the peak positions in fig. 9 for silicon and fig. 10 for the Mylar foils.
Resulting thicknesses are contained in table 2.

	silicon	1 Mylar foil	2 Mylar foils	3 Mylar foils
Thickness d in μm	8.7 ± 0.8	8.5 ± 0.8	16.8 ± 0.8	24.2 ± 0.6

Table 2: Calculated thickness d in μm of the silicon detector and the Mylar foils.

4.1.4 Particle identification

In order to identify the emitted particle their kinetic energy E_{kin} is varied through the use of the Mylar foils. The kinetic energy after the Mylar foils can be calculated by summing the measured quantities ΔE and E.

$$E_{\text{kin}} = E + \Delta E \tag{4.9}$$

Then the count of events can be plotted as a heat map with parameters ΔE and E_{kin} to get the dependency of the energy deposit on the kinetic energy. The result is fig. 11.

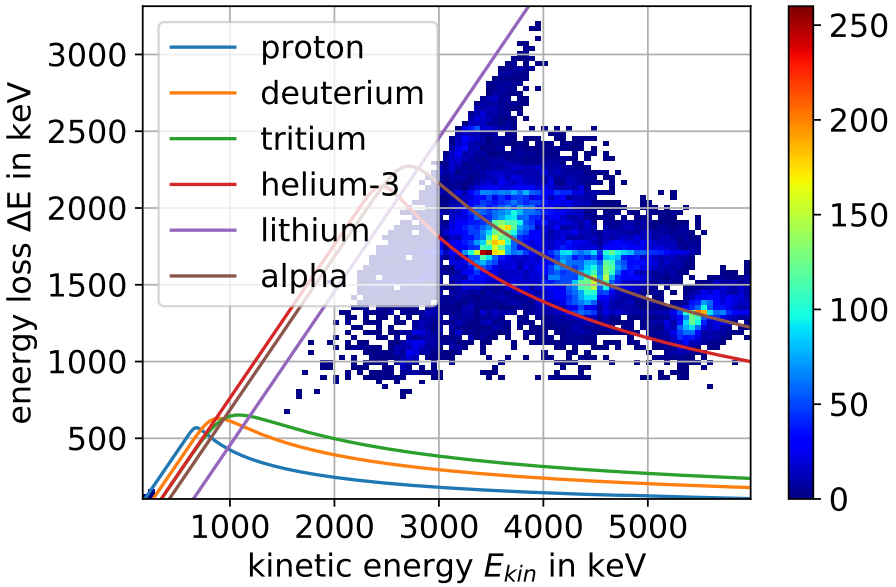

Figure 11: ΔE-E plot. The curves are those expected by the Bethe-Bloch formula for a given particle. The uncertainties of E_{kin} and ΔE can not be included in this representation. (at 4.5 MeV a binning/rounding error occurred due to the way the data was saved (floating-point numbers))

The plot also contains the numerical approximated theoretical curves as predicted by the Bethe-Bloch formula 2.6. The energy-loss is

$$\Delta E = -\int_0^d -\frac{dE}{dx}dx \approx -\sum_i \left(-\frac{dE}{dx}\right)(E_i)\Delta x_i \tag{4.10}$$

where E_i is the remaining kinetic energy after passing a small distance Δx_i in the silicon ΔE-detector. Then the Riemann Sum converges towards the integral for $\Delta x \ll d$. In order to use the Bethe-Bloch formula we need to transform the kinetic energy E_{kin} to relativistic quantities with

$$pc^2 = \sqrt{(E_{\text{kin}} + m)^2 - m^2c^4} \tag{4.11}$$

$$\gamma = \sqrt{1 + \frac{p^2}{m^2}} \tag{4.12}$$

$$\beta = \sqrt{1 - \frac{1}{\gamma^2}}\,. \tag{4.13}$$

The used parameters for the particles are listed in table 3.

particles	charge q in e	mass m in MeV
proton	1	938.272
deuterium	1	1875.61
tritium	1	2809.432
helium-3	2	2809.414
lithium	3	6465.5
alpha	2	3727.379

Table 3: Constants of particles.[4]

Apart from looking at the direct energy-loss dependency we can numerical calculate $\Delta E\beta^2$ for given kinetic energy as in fig. 12.

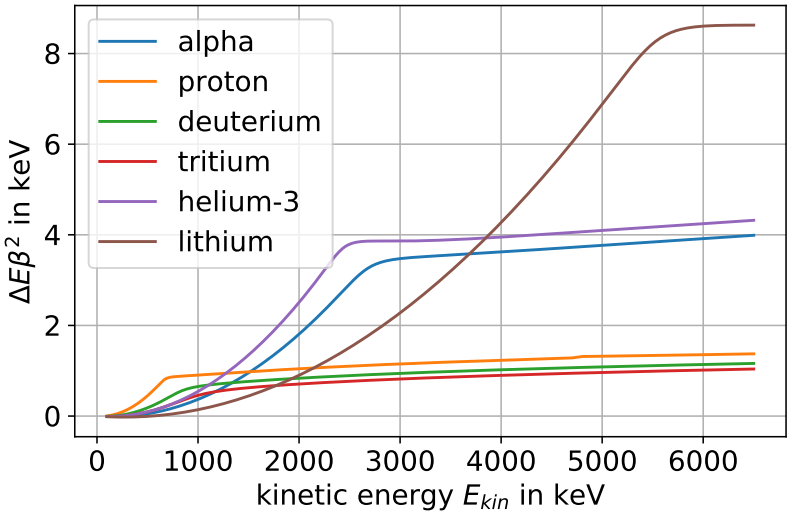

Figure 12: $\Delta E\beta^2$ plot. Expected curves for given particles by the Bethe-Bloch formula.

If the particles were equal distributed in E_{kin} there would be a peak at the $\Delta E\beta^2$ of the approximate plateaus. The measured distribution in E_{kin} is not very constant as seen in fig. 11 but the peak is still visible. The covered energy range is $E_{\text{kin}} \in (2000\,\text{keV}, 6000\,\text{keV})$. Therefore, an approximately constant distribution in $\Delta E\beta^2$ is expected for lithium. For the heavy single charged particles (proton, deuterium and tritium) a clear peak is expected, as the range is only a plateau. For the helium particles also a peak is expected, but with some smearing effects due to the low energy events which are not in the plateau. All plots are listed in the appendix 6.2. The two best fitting curves are of the alpha in fig. 13 and helium-3 in fig. 14 particles.

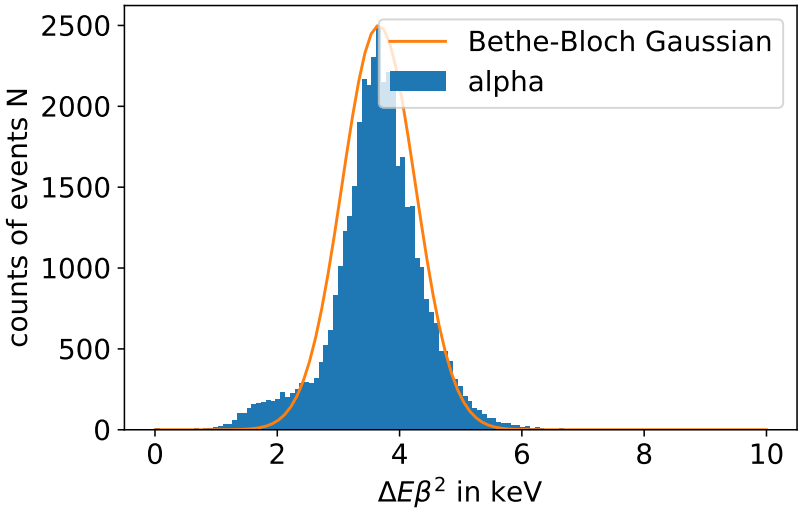

Figure 13: $\Delta E\beta^2$ plot for assumed alpha.

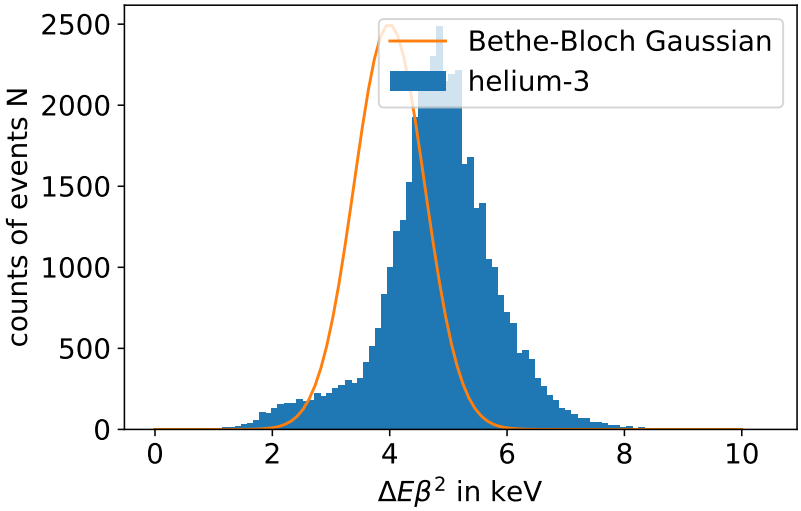

Figure 14: $\Delta E\beta^2$ plot for assumed helium-3.

The blue histogram peak position varies for every particle since β varies with the mass of the particle. The yellow Bethe-Bloch Gaussians are for all particles of constant width but the peak is at the average of $\Delta E\beta^2$ in the range of $E_{\text{kin}} \in (2500\,\text{keV}, 6000\,\text{keV})$. This average approximates the plateau.

4.2 Discussion

At this point it is necessary to review the results and discuss them. Beginning with the determination of thickness of the components. Here it was found that the ΔE-detector has a thickness of $(8.7 \pm 0.8)\,\mu m$ and $(8.5 \pm 0.8)\,\mu m$ for a single Mylar foil. Dividing the result for two and three Mylar foils by their number respectively gives values which lie in the uncertainty of a single foil. This enforces the assumption of a linear approximation in between the given steps in the energy-loss curves.
As for the Bethe-Bloch-plot (see fig. 11) all of the data points are close to the theoretical values especially for helium-3 and more importantly for α-particles. However from the $\Delta E\beta^2$-plots it can be shown, that there is no equal distribution of the kinetic energy for different particles. There can also be seen that the plots for the different particles have a "tail" for lower $\Delta E\beta^2$ which differs from an ideal Gaussian. This stems from the non-plateau values and should be factored out. The Bethe-Bloch Gaussian for α-particles fits almost perfectly with measurements which is to be expected since those particles should primarily be observed. Helium-3 also comes close to this, but there more counts of events which are laying outside the Bethe-Bloch Gaussian. Important to note is that for the determination of thickness of the ΔE-detector α-radiation was assumed, thus this result has to be taken carefully.

5 Conclusion

At the end it can be said that this investigation was successful in terms of the determination of thickness and that the measured data correlates with α-particles.

6 Appendix

6.1 Uncertainties

Any uncertainties will be calculated in accordance with GUM. The equations used for that are seen in (15) and (16). For the calculations the python library "uncertainties" will be used, which follows the guidelines of GUM. As for the uncertainties of specific parameters the approximation curves of the y-uncertainties of those parameters will be regarded and

the method of least squares used. Here the method “scipy.optimize.curve_fit()” from the uncertainties library is taken.

$$x = \sum_{i=1}^{N} x_i; \quad \sigma_x = \sqrt{\sum_{i=1}^{N} \sigma_{x_i}^2}$$

Figure 15: formula for combined uncertainties of the same type after GUM.

$$f = f(x_1, \ldots, x_N); \quad \sigma_f = \sqrt{\sum_{i=1}^{N} \left(\frac{\partial f}{\partial x_i} \sigma_{x_i} \right)^2}$$

Figure 16: formula for propagated uncertainties of first order after GUM.

6.2 $\Delta E\beta^2$ plots

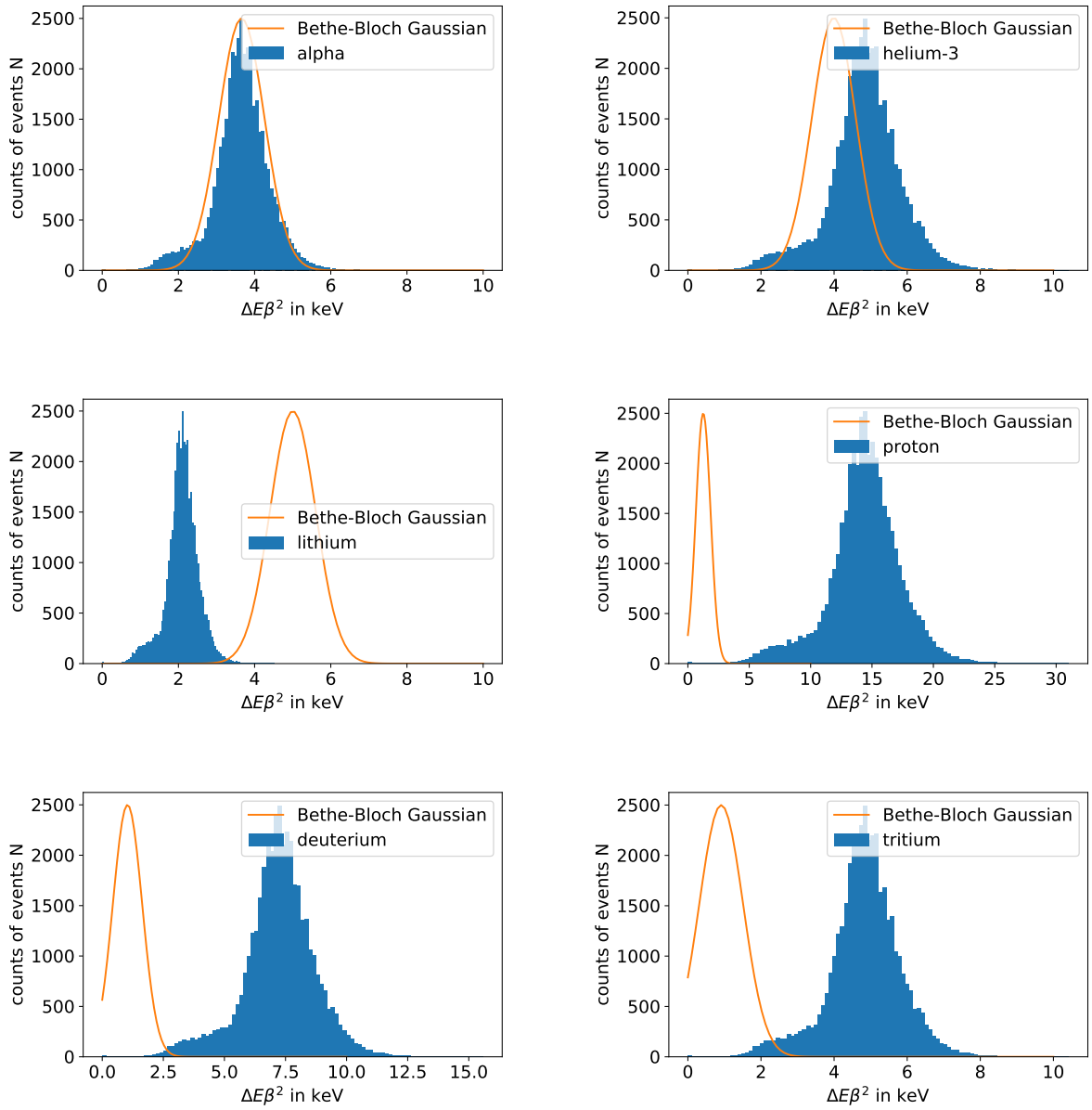

Figure 17: $\Delta E\beta^2$ plots of alpha, helium-3, lithium, proton, deuterium and tritium.

References

[1] Wikipedia. *Alpha-Zerfall*. URL: `https://de.wikipedia.org/wiki/Datei:Coulomb-Barriere.png#/media/File:Coulomb-Barriere.png`.

[2] Octopus in Vitro. *Stopping Power Calculation*. URL: `http://ppsnippets.tk/dosimetry/`.

[3] Institut für Kernphysik Münster. *Anleitung zum Versuch "Teilchenidentifikation mit einem ΔE-E-Aufbau"*.

[4] various Wikipedia entries for the particles listed.